

Supplementary Materials for

Remote picometric acoustic sensing via ultrastable laser homodyne interferometry

Yoon-Soo Jang,^{1,2,3,*}, Dong Il Lee,¹ Jaime Flor Flores,¹ Wenting Wang,^{1,4} and Chee Wei Wong,^{1*}

¹Fang Lu Mesoscopic Optics and Quantum Electronics Laboratory, University of California, Los Angeles, CA 90095, USA.

²Length and Dimensional Metrology Group, Division of Physical Metrology, Korea Research Institute of Standards and Science (KRISS), 267 Gajeong-ro, Yuseong-gu, Daejeon, 34113, Republic of Korea.

³Department of Science of Measurement, University of Science and Technology (UST), Daejeon, 34113, Rep. of Korea.

⁴Communication and Integrated Photonics Laboratory, Xiongan Institute of Innovation, Chinese Academy of Sciences, Xiong'an New Area 071700, China.

* ysj@kirss.ac.kr; cheewei.wong@ucla.edu

This Supplementary Materials consists of the following sections:

Section S1. Effect of laser frequency noise on displacement noise

Section S2. Real-time and long-distance sound and music recording and re-creation

Section S3. Sound detection with pellicle beam splitter

Section S4. Comparison with state-of-the-art acoustic sensing

Section S1. Effect of laser frequency noise on displacement noise

An interferometric phase (θ) of Michelson interferometry generated by distance (L) can be expressed by $\theta = 2\pi \cdot f_{\text{laser}} \cdot (2n_{\text{air}}L)/c_0$, where f_{laser} is the laser frequency, n_{air} is the refractive index of air, c_0 is speed of light in vacuum, and “2” before L denote round-trip optical beam path. Its first-order partial derivatives are then derived as $\Delta\theta = 2\pi \cdot f_{\text{laser}} \cdot (2n_{\text{air}}\Delta L)/c_0 + 2\pi \cdot \Delta f_{\text{laser}} \cdot (2n_{\text{air}}L)/c_0$. The first term on the right side is the variation of the interferometric phase by displacement (ΔL) and the second term on the right side is attributed to fluctuations of the frequency noise (Δf_{laser}). In our study, the frequency noise is not negligible in the phase noise, since we inserted a 40 m fiber delay line to simulate long distance metrology. To verify how laser frequency noise affects the phase noise, the homodyne error signals before and after the stabilization are measured for the Fabry-Perot cavity stabilized ultrastable laser with 1-Hz linewidth and a laser diode with few tens of kHz linewidth. Before the optical path stabilization, the homodyne error signals of ultrastable laser (black) and laser diode (green) are well-matched from 1 Hz to 10 Hz, where environmental drift

is dominant. Above 10 Hz, the homodyne error signal of the laser diode is larger than the ultrastable laser. Although a commercially available laser diode is enough to measure picometer displacement at short ranges [48-52], the ultrastable laser with few Hertz-level linewidth is necessary for long range picometer displacement measurement [53-55].

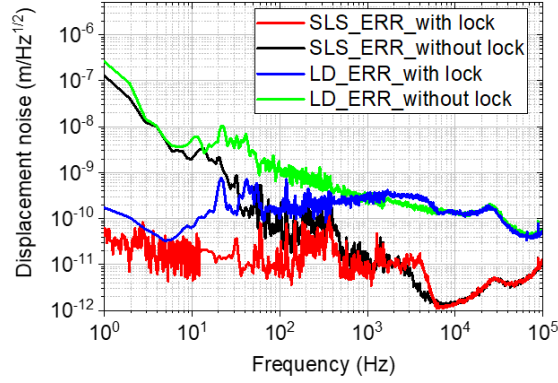


FIG. S1 | Homodyne error signals before and after optical path stabilization. Black and red lines are error signals of the ultra-stable laser before and after optical path stabilization, respectively. Blue and green lines are error signals of the laser diode before and after optical path stabilization, respectively.

Section S2. Real-time and long-distance music recording and re-creation

As shown in Figures 3 and 4 of the main text, our proposed scheme shows feasibility of sound detection at long distance. Figure S2 shows more examples of real-time sound sensing with known acoustic frequencies of 500 Hz and 5 kHz. The control signal is used to measure 500 Hz sounds and the error signal is used to measure 5 kHz sounds. The red lines indicate low-pass filtered data with cutoff frequencies of 1 kHz and 10 kHz respectively. As shown in Figure S2, the low-pass filtered data show clear sinusoidal signals of both control and error signals.

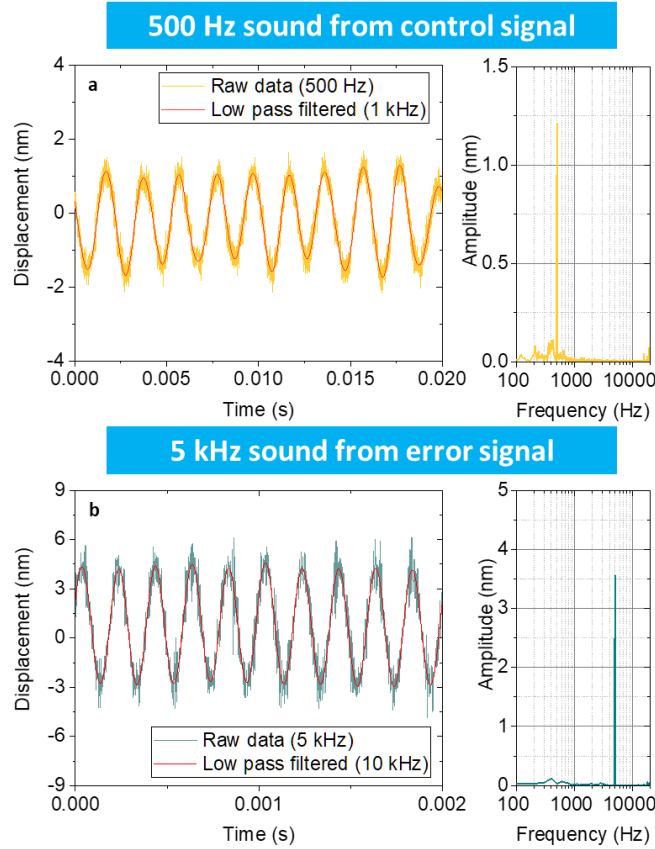


FIG. S2 | Example of real-time acoustic sensing. a, 500 Hz sounds recorded by control signal. **b**, 5 kHz sounds recorded by error signal. Sounds are generated by a portable speaker.

Figure S3 shows impulse responses in the time-domain and its spectrograms. The impulse sound is generated by clapping. The upper panels (**a,c**) are control signal based results and the lower panels (**b,d**) are error signal based results. For the impulse response, the displacement measured by the error signal shows higher frequency components than that measured by control signal because of the bandwidth limitation on control signal. As shown in Figures S3c and d, the error signal based spectrogram shows higher frequency components. Note that if the target has a high-frequency response such as a membrane, it would be possible to measure high-frequency sound over 20 kHz.

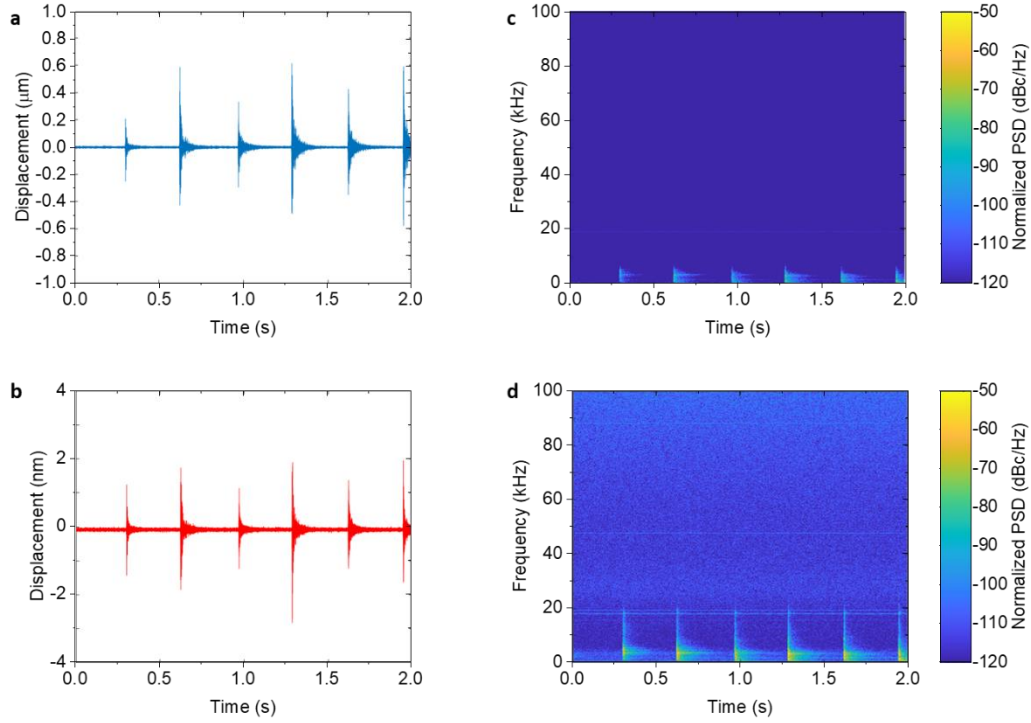


FIG. S3 | Impulse responses and corresponding spectrograms. a-b, Time-domain waveforms of control signal based record measurement (blue) and error signal based record measurement (pink). **c-d,** Spectrograms corresponding to **a-b**, respectively. Impulse-like sound is generated by clapping.

Section S3. Sound detection with pellicle beam splitter

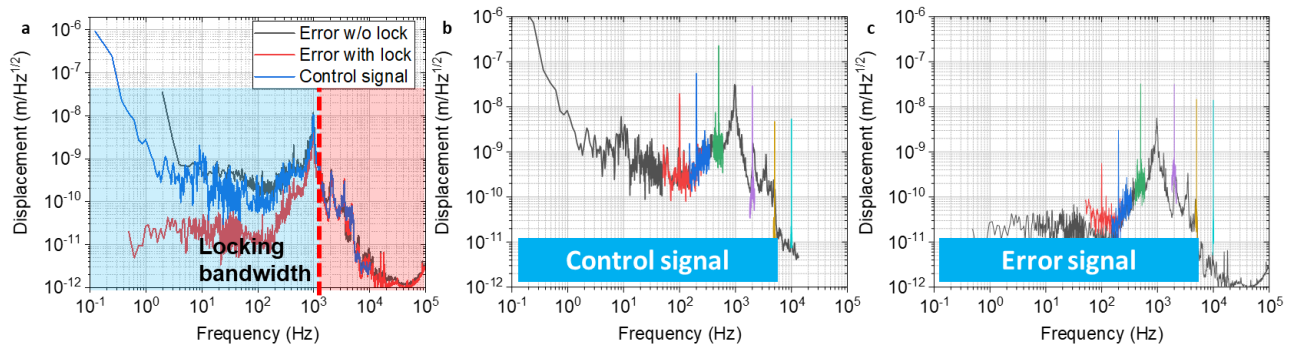


FIG. S4 | Power spectral density of displacement noise for pellicle beam splitter. a, Power spectral density of displacement noise from error signal (red) and control signal (blue) with optical path stabilization using interferometric homodyne signal. **b,** Sound sensing using the control signal. **c,** Sound sensing using the error signal.

Since the pellicle beam splitter has few micrometer thickness, its response to sound and environmental noise is more sensitive than the window case described in main text. Figure S4a shows the typical power spectral density of displacement noise floor on the pellicle beam splitter obtained from error and control signals. Error signal (red line) and control signal (blue line) with optical path stabilization are plotted together, and the error signal without the stabilization is also plotted in gray line. Compared to the window case described in main text, the amplitude of displacement is larger over the whole observation frequency. The peak displacement is hundreds of nanometers and observed near 1 kHz, estimated to be mechanical resonance of the pellicle beam splitter. Figures S4b and S4c show example results of frequency-domain sound sensing from 100 Hz to 10 kHz using the control and error signals. Note that near the 1 kHz, the sound signal is not detectable because the amplitude of sound induced vibration is too large to be detected by our system. From 100 Hz to 500 Hz, the control signal based sound signal is larger than the error signal based sound signal. Over the 2 kHz, the error signal based sound signal is larger than the control signal based sound signal.

Figure S5 shows the mapping of sound intensity-dependent displacement response of the pellicle beam splitter from 100 Hz to 15 kHz. All measurement results of displacement amplitude show linear proportionality to the sound intensities. Since thin film-type devices generate large sound induced vibration, our scheme can be used in voice recognition system [56] and next-generation standard for sound measurement spanning low to high frequencies [57].

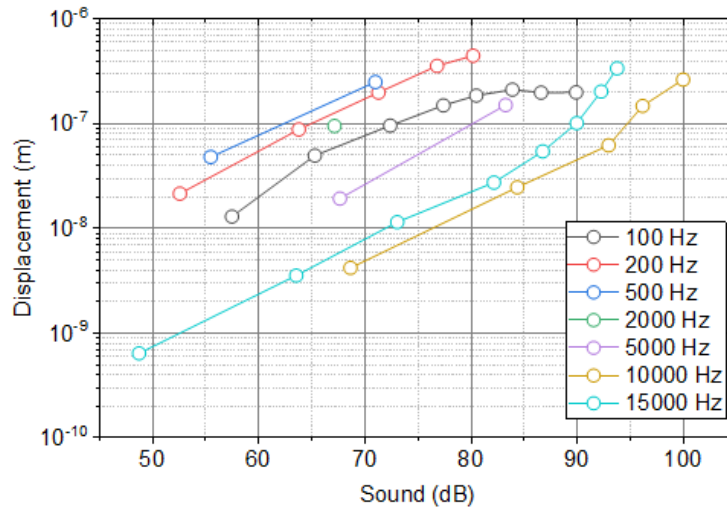


FIG. S5 | Displacement response of the pellicle beam splitter. Measurement results show from 100 Hz to 15 kHz as a function of sound level (dB).

Section S4. Comparison with state-of-the-art acoustic sensing

A table S1 present a performance comparison with state-of-the-art acoustic sensing techniques.

Table S1. Summary Comparison between State-of-the-Art acoustic sensing techniques and our proposed system

Ref.	Metrology approach	Detectable sound frequency	Detectable sound level	Distance range
[30]	Optical microresonators	< 40 MHz	N.A.	Contact-based measurement
[32]	Optomechanical sensor	< 357 kHz	12 - 134 dB @ 315 kHz	Contact-based measurement
[56]	Graphene film based sensor	20 Hz – 20 kHz	N.A.	Contact-based measurement
[57]	Standard microphone	20 Hz – 12.5 kHz	11 – 146 dB	Contact-based measurement
[58]	Polarization dependent reflection of laser	<137.2 MHz	158 – 187 dB @ 1 MHz	Contact-based measurement
[59]	Speckle pattern imaging	220 Hz	N.A.	300 m
[60]	Laser feedback interferometry	200 Hz – 3 kHz	N.A.	200 m
[61]	Acoustic metamaterial	3 kHz – 10 kHz	N.A.	Contact-based measurement
This work	Laser homodyne interferometry with phase locking	< 100 kHz (Dependent on spectrum analyzer)	42 – 140 dB @ 2 kHz, behind window	60 m